Cerebral Cortex February 2008;18:397-406
doi:10.1093/cercor/bhm074
Advance Access publication June 4, 2007

Monosynaptic Connections between Pairs of L5A Pyramidal Neurons in Columns of Juvenile Rat Somatosensory Cortex

Andreas Frick[1], Dirk Feldmeyer[1,2], Moritz Helmstaedter[1] and Bert Sakmann[1]

[1]Abteilung Zellphysiologie, Max-Planck-Institut für Medizinische Forschung, D-69120 Heidelberg, Germany and [2]Department of Medicine, Research Centre Juelich, Institute of Neuroscience and Biophysics INB-3, D-52425 Juelich, Germany

Layer 5 (L5) of somatosensory cortex is a major gateway for projections to intra- and subcortical brain regions. This layer is further divided into 5A and 5B characterized by relatively separate afferent and efferent connections. Little is known about the organization of connections within L5A of neocortical columns. We therefore used paired recordings to probe the anatomy and physiology of monosynaptic connections between L5A pyramidal neurons within the barrel columns of somatosensory cortex in acute slices of ~3-week-old rats. Post hoc reconstruction and calculation of the axodendritic overlap of pre- and postsynaptic neurons, together with identification of putative synaptic contacts (3.5 per connection), indicated a preferred innervation domain in the proximal dendritic region. Synaptic transmission was reliable (failure rate <2%) and had a low variability (coefficient of variation of 0.3). Unitary excitatory postsynaptic potential (EPSP) amplitudes varied 30-fold with a mean of 1.2 mV and displayed depression over a wide range of frequencies (2–100 Hz) during bursts of presynaptic firing. A single L5A pyramidal neuron was estimated to target ~270 other pyramidal neurons within the same layer of its home barrel column, suggesting a mechanism of feed-forward excitation by which synchronized single action potentials are efficiently transmitted within L5A of juvenile cortex.

Keywords: barrel cortex, cortical connectivity, layer 5A, short-term dynamics, synaptic transmission

Introduction

Cortical columns are structural and functional units that link cellular and higher functions of the brain and are common to all areas of the mammalian neocortex (Nelson 2002; Douglas and Martin 2004). One of the cardinal problems in cortical physiology is to elucidate the cellular connectivity within cortical columns and their functional organization depending on task and region. To obtain this knowledge, one needs to identify the cortical cell types involved and to establish the wiring patterns and the properties of the synaptic connections between them. In rodents, the region of primary somatosensory cortex that processes whisker-related information comprises cortical columns representing predominantly individual whiskers. These columns are called barrel columns and include the cortical area above and below layer 4 (L4) barrels from pia to white matter (Woolsey and van der Loos 1970).

Layer 5 (L5) of the barrel cortex receives inputs from several subcortical regions and all cortical layers and, in turn, constitutes a major output to intra- and subcortical targets (Wise and Jones 1977; Killackey et al. 1989; Bernardo, McCasland, and Woolsey 1990; Bernardo, McCasland, Woolsey, and Strominger 1990; Koralek et al. 1990; Ito 1992; Hoeflinger et al. 1995; Gottlieb and Keller 1997). The division of this layer into sublayers 5A and 5B is based on histological and functional differences in the morphology of pyramidal neurons and the afferent and efferent connections (Wise and Jones 1977; Zilles and Wree 1995; Ahissar et al. 2001; Manns et al. 2004; Larsen and Callaway 2006). Receptive fields (RFs) for whisker-evoked responses, for instance, are narrower for L5A pyramidal neurons than for L5B pyramidal neurons as revealed by in vivo recordings (Manns et al. 2004). Tactile sensory information from thalamus reaches L5A pyramidal neurons along 2 parallel projections: from ventral posteromedial thalamic nucleus (VPM, lemniscal pathway) via L4 (Feldmeyer et al. 2005; Schubert et al. 2006) and from posterior thalamic nucleus (POm, paralemniscal pathway) (Koralek et al. 1988; Chmielowska et al. 1989, Lu and Lin 1993; Kim and Ebner 1999; Ahissar and Kleinfeld 2003; Bureau et al. 2006). This convergence of lemniscal and paralemniscal pathways enables L5A pyramidal neurons to integrate different aspects of whisker-related information at an early stage of cortical signal processing. In turn, L5A pyramidal neurons project to the caudate nucleus and several intracortical areas including secondary somatosensory and motor cortices (Donoghue and Parham 1983; Chmielowska et al. 1989; Koralek et al. 1990; Mercier et al. 1990; Lu and Lin 1993; Alloway et al. 1999, 2004; Hoffer et al. 2005).

This study is part of an effort to elucidate the stream of excitation within and across the different layers of a neocortical column in response to a brief whisker deflection. To our knowledge, this is the first study of cellular connectivity within the microcircuits of L5A. We describe the existence of monosynaptic connections between slender-tufted L5A pyramidal neurons and correlate synaptic physiology and anatomical properties for this connection. Based on these data, an estimate for the functional connectivity within the local L5A microcircuits of a whisker-related barrel column is provided. Our results suggest that the physiology and anatomy of these connections may enable a network of slender-tufted L5A pyramidal neurons to contribute to intralayer feed-forward excitation.

Methods

Preparation of Slice and Extracellular Solutions

Wistar rats (18–20 days old) were anesthetized using isoflurane, decapitated, and coronal or thalamocortical slices (350 μm thick) were prepared from the whisker-related "barrel field" of the somatosensory cortex. Experimental procedures were approved by the Animal Research Committee of the Max Planck Society and complied with the guidelines laid out in the EU directive on animal welfare. Brain slices were incubated in an extracellular solution containing (in mM) the following: 125 NaCl, 25 $NaHCO_3$, 2.5 KCl, 1.25 NaH_2PO_4, 6 $MgCl_2$, 1 $CaCl_2$, 3 myo-inositol, 2 Na-pyruvate, 0.4 ascorbic acid, and 25 glucose.

The extracellular solution used for recording contained 125 mM NaCl, 25 mM $NaHCO_3$, 2.5 mM KCl, 1.25 mM NaH_2PO_4, 1 mM $MgCl_2$, 2 mM $CaCl_2$, and 25 mM glucose and was saturated with 95% O_2/5% CO_2 (pH 7.4). All recordings were made at 32–35 °C. Where specified, one or more of the following drugs was added to the bathing solution: D,L-2-Amino-5-phosphonovaleric acid (50 μM) and 2,3-Dioxo-6-nitro-1,2,3,4-tetrahydrobenzo[f]quinoxaline-7-sulfonamide (3–5 μM).

Cell Identification and Electrophysiology

The whisker-related barrel field in L4 of the somatosensory cortex was detectable at low magnification (2.5×) under bright-field illumination (Fig. 1*A*). Neurons were visualized employing differential interference contrast microscopy using a Zeiss Axioskop I microscope fitted with a 60×/0.90 numerical aperture water-immersion objective (Olympus, Hamburg, Germany). Recording pipettes (4–6 MΩ) were pulled from borosilicate glass and filled with the following solution (in mM): 135 K-gluconate, 10 4-(2-hydroxyethyl)-1-piperazineethanesulfonic acid, 10 phosphocreatine-Na, 4 KCl, 4 ATP-Mg, and 0.3 guanosine triphosphate, pH 7.2 (adjusted with KOH). Biocytin (1.5–2.5 mg/mL, Sigma, Munich, Germany) was included in the recording solution to allow post hoc staining and morphological reconstruction of the neurons. Monosynaptic connections were established by probing presynaptic partners using the "loose-seal" technique while recording from the postsynaptic neuron in whole-cell configuration (Feldmeyer et al. 1999). In short, in the loose-seal configuration, the injection of brief (2.5–5 ms) and large (7–10 nA) current pulses triggers action potentials (APs), evoking EPSPs in target neurons. The projecting neuron was then repatched using the whole-cell configuration. Signals were recorded using Axoclamp-2B and Axopatch 200B amplifiers (Axon Instruments, Union City, CA), low-pass filtered at 3 kHz, and sampled at 10–50 kHz. Traces were acquired and analyzed using commercial software (Igor Pro; WaveMetrics, Lake Oswego, OR) with in-house algorithms. To quantify short-term dynamics of synaptic transmission, we triggered bursts of 3–5 APs at interspike intervals (ISIs) ranging from 10 to 500 ms in the projecting neuron and calculated the paired-pulse ratio (PPR) of the EPSP amplitudes ($EPSP_X$/$EPSP_1$, X denotes the position of the EPSP during a burst). In order to prevent false results (for instance due to response failures), we first averaged the amplitudes for $EPSP_1$, $EPSP_2$, $EPSP_3$, and $EPSP_5$ and then calculated the PPR values. Group data are expressed as mean ± standard deviation unless otherwise stated, and statistical significance was calculated using nonparametric statistical tests (Mann–Whitney test).

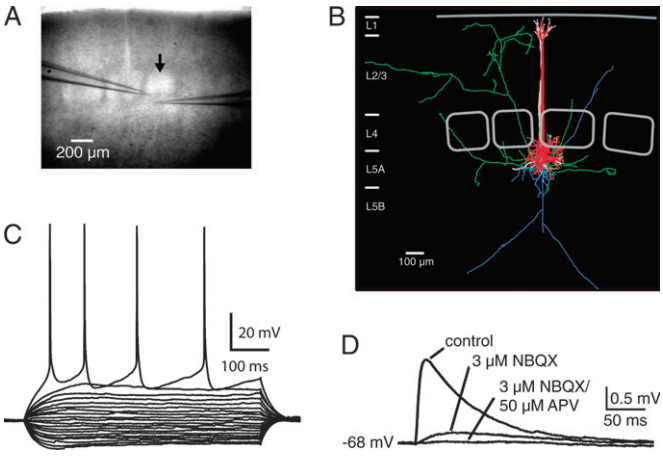

Figure 1. Monosynaptic connections between L5A pyramidal neurons in the barrel cortex of rats. (*A*) IR-differential interference contrast image of "barrels" and of a pair of synaptically connected L5A–L5A pyramidal neurons just beneath L4 (barrel marked by arrow). (*B*) Neurolucida reconstruction of a synaptically connected pair of L5A pyramidal neurons from a P18 animal. The dendritic and axonal arbors of the presynaptic (red and blue, respectively) and postsynaptic (white and green, respectively) neuron are shown. The distance of the cell bodies from the pia was ~870 μm. (*C*) Regular AP firing of a L5A pyramidal neuron during current injection. (*D*) The postsynaptic responses are blocked by the ionotropic glutamate receptor antagonists NBQX (3 μM) and D,L-APV (50 μM).

Staining

After recording, biocytin-filled neurons were processed using standard procedures described previously (Feldmeyer et al. 2005). Slices were fixed at 4 °C for at least 24 h in phosphate-buffered saline containing 4% paraformaldehyde and then incubated in 0.1% Triton X-100 solution containing avidin-biotinylated horseradish peroxidase (ABC-Elite; Camon, Wiesbaden, Germany). Subsequently, 3,3-diaminobenzidine was used as reactive chromogen until axons and dendrites were clearly visible (after 2–4 min). To enhance staining contrast, slices were occasionally postfixed in 0.5% OsO_4 for 30–40 min before mounting on slides and embedding using Moviol (Clariant, Sulzbach, Germany).

Histology

Neurons were reconstructed using Neurolucida software (MicroBright-Field, Colchester, VT) using an Olympus Optical (Hamburg, Germany) BX50 microscope equipped with a 100× objective (Lübke et al. 2003). No corrections for shrinkage were made. The reconstructions provided the basis for quantification of 1) the location of the neurons with respect to the barrels, 2) the number and location of putative synaptic contacts between pairs, 3) the density of axonal boutons, and 4) the axonal and dendritic arborization in the different layers of the cortical columns. Axonal boutons and putative synaptic contacts were identified under the light microscope at a final magnification of 1000× (100× oil immersion lens and 10× eyepiece). Putative synaptic contacts were defined as close appositions of presynaptic axonal boutons and postsynaptic spines in the same focal plane (see Fig. 3). To calculate the density of axonal boutons for an estimate of anatomical connectivity, six ~50-μm sections of axons within the innervation domain were selected from 3 different presynaptic neurons each. The estimation of the total number of boutons in a particular layer and column was calculated by multiplying the measured density by the total length of axons for that corresponding region.

Innervation Domains

Calculation of axonal and dendritic density maps and innervation domains has been described in detail elsewhere (Lübke et al. 2003). Reconstructions of neuronal morphologies were aligned in the plane of the slice with respect to the home barrel center (barrels were identified in low-power bright-field micrographs from the acute brain slices). The dendritic and axonal path length was integrated in 50-μm voxels in the plane of the slice, yielding a 2D map of "length density." The raw density maps were then spatially low-pass filtered by 2D convolution with a Gaussian kernel (σ =50 μm), and continuous 2D density functions were constructed using bicubic interpolation in custom-made software package "Rembrandt I" programmed in IGOR Pro (WaveMetrics). To calculate the putative "innervation domain" between pairs of L5A pyramidal neurons, these axonal and dendritic length density maps were multiplied in each voxel; "80% domains" were given as isodensity contours containing 80% of the total path length.

Results

Dual whole-cell recordings were made from 27 synaptically coupled pairs of L5A pyramidal neurons. L5A pyramidal neurons were distinguished from L5B pyramidal neurons in living brain slices based on 1) their laminar localization within the band between L4 and L5B (Fig. 1*A*) and 2) their neuronal morphology, which is characterized by a relatively small cell body and a slender apical dendrite (Fig. 1*B*) (Feldmeyer et al. 2005; Schubert et al. 2006). We also determined the biophysical properties of the selected neurons, including their current–voltage relation, AP firing properties, and input resistance (R_{in}). Figure 1*C* shows an overlay of membrane voltage responses to injections of 600-ms-long negative and positive current pulses of varying amplitudes through the whole-cell pipette. Hyperpolarizing current injections induced typical sag responses, and suprathreshold depolarizations led to regular spiking patterns. Few neurons (~8%) responded to rheobase injections with a doublet of APs at high interburst frequencies of 137–250 Hz.

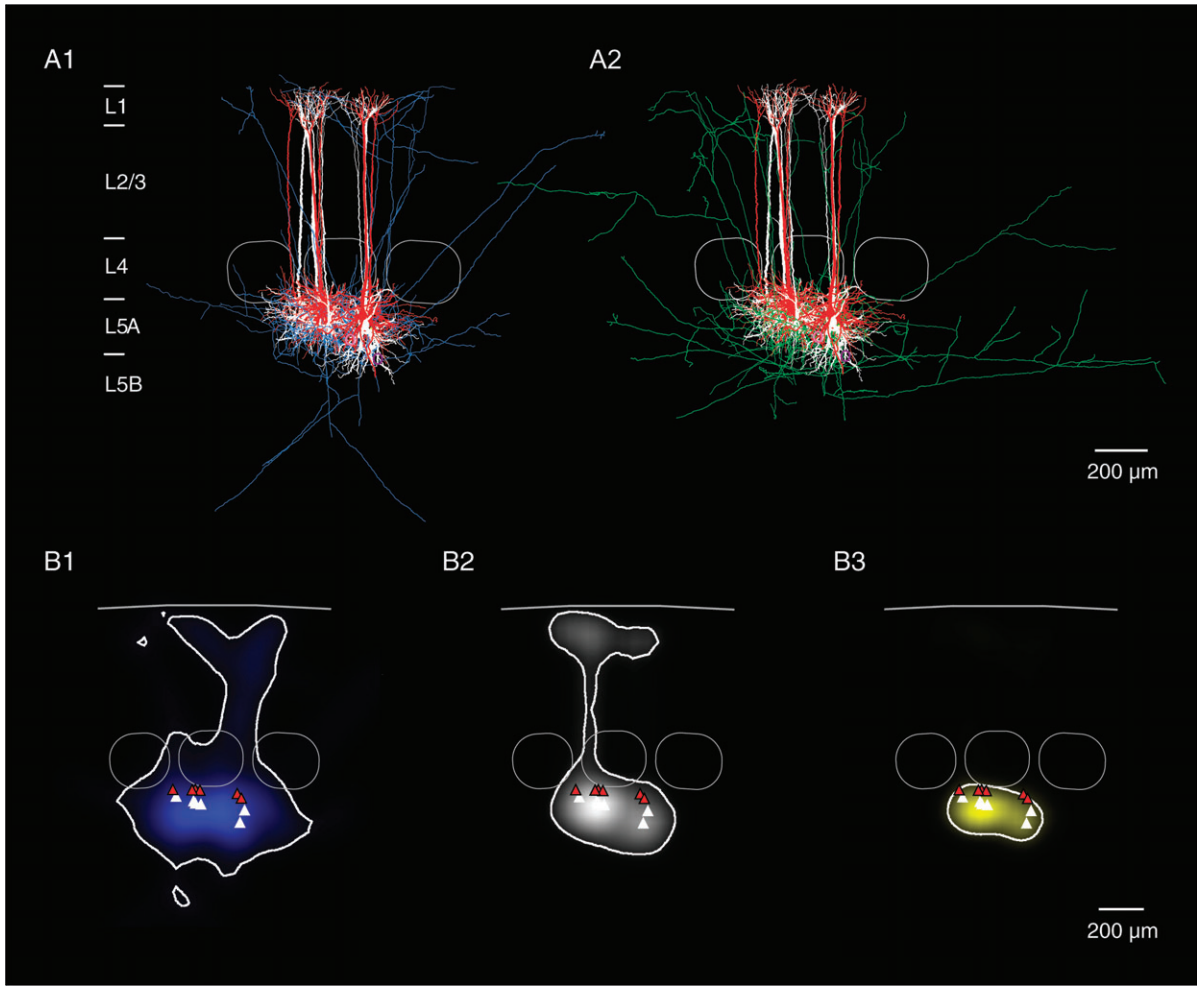

Figure 2. Overlay and density maps of synaptically coupled L5A pyramidal neuron pairs. (*A*) Barrel-centered overlay of the Neurolucida reconstructions of 6 synaptically coupled L5A pyramidal pairs. Connections were found almost exclusively between neurons located at the barrel borders. The average center barrel and 2 neighboring barrels are outlined in white. (*A1*) Superposition of presynaptic axons (blue) and postsynaptic dendrites (white). The presynaptic dendrites (red) are shown as well. (*A2*) Superposition of postsynaptic axons (green; postsynaptic dendrites in white) and presynaptic dendrites (red). Note that the axons of L5A pyramidal neurons project into different layers and adjacent barrel columns. (*B*) 2D maps of presynaptic axonal (*B1*) and postsynaptic dendritic (*B2*) length density of the same synaptically coupled pairs aligned with respect to the center of the barrel. The predicted innervation domain (*B3*) is calculated as the product of axonal and dendritic densities. Contour lines enclose 80% of the integrated density. The presynaptic neurons (red triangles) were typically located closer to L4 and the postsynaptic ones closer to L5B (white triangles).

The input resistance averaged 90 ± 31 MΩ (n = 31), ranging from 53 to 173 MΩ (Table 2).

Characterization of Monosynaptic Connections

To characterize the physiological properties of monosynaptic connections between L5A pyramidal neurons, we measured peak amplitude, latency, time course, and failure rate of unitary EPSPs. Unitary EPSPs were evoked in the target neuron by triggering single or bursts of 3–5 APs in the projecting neuron using intracellular current injection. This stimulation pattern was repeated 40–200 times at rates of 0.05–0.1 Hz (every 10–20 s), at which there was no obvious rundown of the EPSP amplitude (see Fig. 6*B*). The majority (23 out of 27) of L5A–L5A connections was unidirectional and only a small percentage (~15%) bidirectional. Unitary EPSPs were mediated by ionotropic glutamate receptors and completely blocked by bath application of the α-Amino-3-hydroxy-5-Methyl-4-isoxazolephropionic acid and N-Methyl-D-aspartic acid receptor blockers NBQX (3–5 µM) and D,L-APV (50 µM), respectively (n = 4, Fig. 1*D*).

Axonal and Dendritic Arborization

The morphological reconstruction of a pair of synaptically connected L5A pyramidal neurons is shown in Figure 1*B*. In this and the following figures, dendrites and axons of presynaptic neurons are depicted in red and blue, respectively, and dendrites and axons of postsynaptic neurons in white and green, respectively. To quantify the geometry of their axonal and dendritic arbors and for identification of putative synaptic contacts between them, we carried out a detailed morphological reconstruction of 6 pairs of connected L5A pyramidal neurons. Figure 2 shows an overlay of the 2D projections of these pairs centered with reference to the averaged barrel outlines. This analysis revealed that cell bodies of connected pairs were located at the lateral border of their respective barrel column and showed a clear tendency toward a vertical clustering (6 out of 6). The cell bodies of the presynaptic neurons were closer to the L4–L5A border (distance 29 ± 22 µm) and separated from the postsynaptic ones by 67 ± 35 µm (range 33–135 µm, Table 1). Dendrites of L5A pyramidal neurons were divided into basal and apical dendritic arbors and had an average

Table 1
Morphological characteristics of rat L5A pyramidal neurons

Cell identity	Distance (μm)			Dendritic length (μm)						No. of primary dendrities	
	To barrel	Pre-post	To pia	Total	Basal	Apical				Basal	Oblique
						Main	Oblique	Tuft in L1	Total		
1_pre	19	33	898	6437	3572	1053	1428	385	2865	4	3
1_post	52		931	4917	1951	1304	590	1071	2966	5	5
2_pre	71	55	931	6925	4077	979	966	902	2848	6	6
2_post	126		920	5240	2586	947	802	904	2654	6	6
3_pre	27	63	936	5400	3930	1002	407	62	1471	5	1
3_post	90		999	8096	3974	1143	2587	392	4122	8	2
4_pre	24	135	876	8946	6011	1250	1044	640	2935	6	4
4_post	159		1011	7472	3692	1685	1697	418	3780	7	6
5_pre	26	65	869	5709	2832	794	1331	752	2877	4	4
5_post	90		933	5796	2207	1275	1882	431	3588	8	4
6_pre	9	54	864	5288	1920	1442	1462	485	3368	4	6
6_post	63		918	8587	4047	1587	2669	284	4540	6	6
Mean	63	67	918	6568	3400	1203	1405	559	3168	5.8	4.4
Standard deviation	47	35	49	1410	1172	267	718	297	792	1.4	1.7
Median	57	59	919	6116	3632	1196	1379	448	2950	60.0	4.5
Minimum	9	33	864	4917	1920	794	407	62	1471	4	1
Maximum	159	135	1011	8946	6011	1665	2669	1071	4540	8	6
% Total dend length				100	51	19	21	9	46		

total length of 6568 ± 1410 μm per neuron (100%, n = 12, Table 1). Seventy percent of the dendrites were confined to the home barrel column, increasing to 90% when the neighboring septa were included. The average total length of the basal dendritic tree (number of basal dendrites: 5.8 ± 1.4) was 3400 ± 1172 μm (51% of all dendrites), extended laterally to about the width of a barrel (300–400 μm), and was largely confined to L5 and lower L4. The apical dendritic arbor (3168 ± 792 μm, 49% of all dendrites) spanned 918 ± 49 μm from cell body to pia (range 864–1011 μm, Table 1) and was further subdivided into main, oblique, and tuft dendrites. Structurally, the main apical dendrite was slender, giving rise to few (4.4 ± 1.7) oblique dendrites (1405 ± 718 μm, 21% of all dendrites) mainly proximally to the soma in L5A and lower L4, and extending into a small tuft largely confined to L1 (559 ± 297 μm, 9%). The axons of L5A pyramidal neurons (total length 7819 ± 2491 μm) projected vertically toward layer 1 and the white matter, as well as horizontally into neighboring cortical columns within layers 5, 4, and 2/3 (Fig. 2*A1*,*A2*). The axonal domain of the presynaptic neurons was very dense in the vicinity of the postsynaptic cell bodies suggesting a high local connectivity there (see below).

Innervation Domain and Putative Synaptic Contacts

To assess the target region where L5A pyramidal neurons might form synaptic contacts with each other (the innervation domain), we computed the overlap of presynaptic axons and postsynaptic dendrites (Fig. 2*A*). For this analysis, 2D maps were computed from the 3D reconstructions of the respective axonal (Fig. 2*B1*) and dendritic (Fig. 2*B2*) length densities, and the predicted innervation domain was then calculated as the product of these densities. Figure 2*B3* shows the contour lines delimiting 80% of the integrated density. These data suggest that synaptic contacts are mainly located on the basal dendrites and to a lesser degree on the proximal oblique dendrites and that the target regions are essentially columnar. A better estimate for the location and number of putative synaptic contacts can be achieved by scanning for close approximations of axons and dendrites under light microscopy at high (1000×) magnification (Fig. 3). For 6 reconstructed L5A pyramidal neuron pairs, the mean number of putative synaptic contacts per monosynaptic connection was 3.5 ± 1.8 ranging from 1 to 6 (Fig. 4*A*, Table 2). The geometric distance of these putative

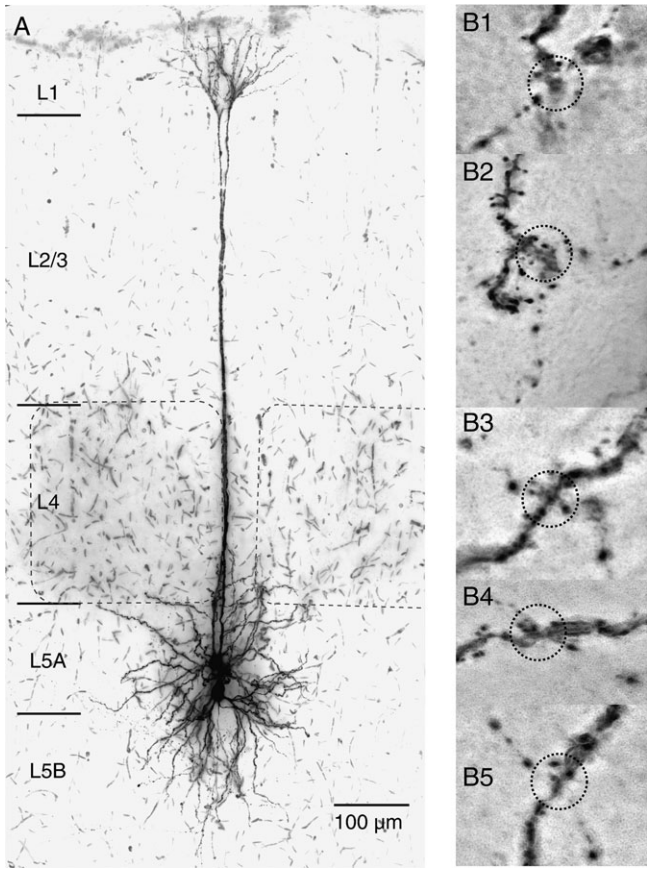

Figure 3. Putative synaptic contacts of a monosynaptic L5A–L5A connection. (*A*) Biocytin staining of a L5A–L5A pyramidal neuron pair from a P18 animal. Photograph of a synaptically connected pair. Barrels are indicated by dashed lines. For this connection, 5 putative synaptic contacts were identified by light microscopy. (*B1–B5*) Higher magnification of these putative contacts. Images were improved using deconvolution algorithms.

contacts from the soma was between 13 and 264 μm averaging 107 ± 63 μm (Fig. 4*B*). The majority (66.6%) was found on basal dendrites at a mean distance of 84 ± 43 μm, a smaller fraction (33.3%) on proximal oblique dendrites at a distance of 152 ± 74 μm, and none in the terminal tuft dendrites. This analysis complements the information gained from the calculated innervation domain.

Properties of Unitary EPSPs

Synaptic properties of monosynaptic L5A–L5A connections were derived from the analysis of unitary EPSPs evoked in the target neuron in response to APs triggered in the projecting neuron. The results from one experiment are illustrated in Figure 5. Unitary EPSPs (Fig. 5*A*, upper traces) fluctuated in peak amplitude and onset latency during successive trials. The reconstruction of this L5A–L5A pair revealed 6 potential synaptic contacts located at different geometric distances from the soma (69–264 μm; average 160 ± 70 μm) and is shown in Figure 5*B*. The EPSP onset latency histogram (Fig. 5*C*) had a single peak and was negatively correlated with amplitude (Fig. 5*D*). This connection had mean unitary EPSP amplitude of 1.2 ± 0.3 mV and was highly reliable (failure rate 0%, $n = 60$ responses).

The results from 27 similar experiments are summarized in Figure 6 and Table 2. Unitary EPSP amplitudes evoked by single APs varied 30-fold for different connections of this population, ranging from 0.19 to 6.26 mV with an average of 1.24 ± 1.28 mV (Fig. 6*A*). The latency between the peak of the AP and the EPSP onset ranged from 0.5 to 1.9 ms and was on average 1.1 ± 0.4 ms. Rise times (20–80% of the peak amplitude) and decay time constants were 1.2 ± 0.5 ms and 17.8 ± 4.5 ms, respectively. Synaptic transmission between L5A pyramidal neurons was highly reliable, resulting in a low coefficient of variation (CV) of unitary EPSPs that ranged from 0.11 to 0.73 with a mean of 0.30 ± 0.16 (Fig. 6*B*). This result suggests a relatively high release probability at monosynaptic L5A–L5A connections. The CV was inversely related to the EPSP amplitude (Fig. 6*C*) as described previously for several neocortical connections (Markram et al. 1997; Feldmeyer et al. 1999, 2006). Calculations of limiting curves assuming binomial release with

$$\mathrm{CV} = \sqrt{\frac{1 - p_r}{n_b \cdot p_r}} \quad \text{and} \quad p_r = \frac{\Delta V}{n_b \cdot q_s}$$

and fixed values for the number of release sites n_b and the quantal amplitude q_s were not satisfactory because EPSP amplitudes larger than 2.0 mV were not included. To obtain limits for n_b and q_s, an n_b of 4 was assumed (close to the mean number of putative synaptic contacts, see Fig. 4*A* and Table 2). The 2 limiting curves in Figure 6*C* were calculated for $q_s = 0.10$ and 0.55 mV. The range of quantal EPSP amplitudes is similar to that observed for intralaminar connections between L2/3 pyramidal cells, smaller than that estimated for L4–L4 and L5B–L5B connections, but larger compared with that for L4–L2/3 connections (Markram et al. 1997; Feldmeyer et al. 1999, 2002, 2006). Failures occurred infrequently (range 0–12.4%, mean 1.4 ± 3.3%), were more common for "weak" connections (mean EPSP amplitude < 0.5 mV) but even then did not exceed 12%; ~80% of the connections (18 out of 22) showed virtually no failures (i.e., less than 2%), again emphasizing the reliability of this connection.

Short-Term Changes of Synaptic Efficacy

We next wanted to address the question of how bursts of APs occurring in the barrel cortex in vivo (Armstrong-James et al. 1994; Huang et al. 1998; Brecht and Sakmann 2002; Wilent and Contreras 2004) affect the efficacy of synaptic transmission in this local network. Therefore, we measured the short-term changes of synaptic responses to a burst of 3 APs at ISIs of 100 ms (Fig. 7, Table 2). At this rate, temporal summation, which would otherwise confound our analysis (Banitt et al. 2005), is minimal, while it is well within the range of ISIs resulting in short-term changes of synaptic transmission (up to ~1 s; Zucker and Regehr 2002). A representative example for the short-term changes is illustrated in Figure 7*A,B*. Six successive postsynaptic responses to short trains of 3 APs triggered in the presynaptic neuron (upper trace), and the average response of 30 successive sweeps (bottom trace) are shown in Figure 7*A*. We found a PPR (see Methods) for the second EPSP amplitude of 82% and for the third EPSP amplitude of 66%, indicating strong depression of synaptic efficacy during bursts of APs. For this particular connection, the amplitude values for the second and third EPSP ($EPSP_2$ and $EPSP_3$) are plotted against the amplitude values of the first EPSP ($EPSP_1$) for 30 consecutive sweeps,

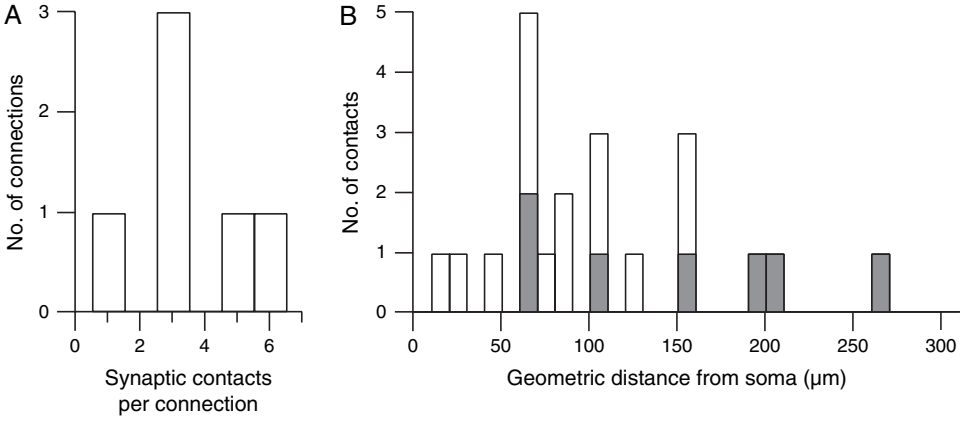

Figure 4. Putative synaptic contacts between L5A pyramidal neurons. Histograms of the number of putative contacts per connection (*A*) and the geometrical distance of putative synaptic contacts from cell body (*B*) analyzed for 6 completely reconstructed pairs of L5A pyramidal neurons. Contacts on apical oblique dendrites are shown in gray to distinguish them from those on the basal dendrites (white).

demonstrating synaptic depression and variability during bursts of activity. To further probe the frequency dependence of synaptic transmission, we recorded bursts of 3–5 APs at ISIs ranging from 10 to 500 ms (Fig. 7*C*,*D*; $n = 9$). Depression of synaptic transmission occurred at all frequencies tested and was particularly prominent at high frequencies (50–100 Hz). The relation between PPR (i.e., the ratio of $EPSP_2$, $EPSP_3$, and $EPSP_5$ relative to $EPSP_1$) and ISI is plotted in Figure 7*D*. For the 10 ms ISI, $EPSP_2$ was 0.48 ± 0.07 ($n = 7$), $EPSP_3$ 0.27 ± 0.05 ($n = 7$), and $EPSP_5$ 0.10 ± 0.06 ($n = 4$). For 200 and 500 ms ISIs (data not shown), short-term depression was similar to that for 100 ms.

Table 2
Properties of synaptic connections and input resistance (mean ± standard deviation)

Unitary EPSP (mV)	1.24 ± 1.28 ($n = 27$)
CV	0.30 ± 0.16 ($n = 26$)
Failure rate (%)	1.4 ± 3.3 ($n = 22$)
PPR (%) ($EPSP_2/EPSP_1$)	82 ± 10 ($n = 20$)
PPR (%) ($EPSP_3/EPSP_1$)	67 ± 10 ($n = 20$)
20–80% Rise time (ms)	1.23 ± 0.47 ($n = 20$)
Decay time constant (ms)	17.8 ± 4.5 ($n = 18$)
Latency (ms)	1.07 ± 0.40 ($n = 20$)
Synaptic contacts	3.5 ± 1.8 ($n = 6$)
Input resistance (M)	90 ± 31 ($n = 31$)

Discussion

In this study, we established the existence of monosynaptic connections between slender-tufted L5A pyramidal neurons and correlated the structural determinants of their connectivity with their physiological properties. Knowledge from this and related studies is aimed at understanding the neuronal basis and wiring of neocortical columns to elucidate the stream of excitation within them.

Intra- and Subcortical Connections of L5A Pyramidal Neurons

Whisker-related sensory signals are relayed from thalamus to neocortex along 2 parallel pathways, namely, the lemniscal

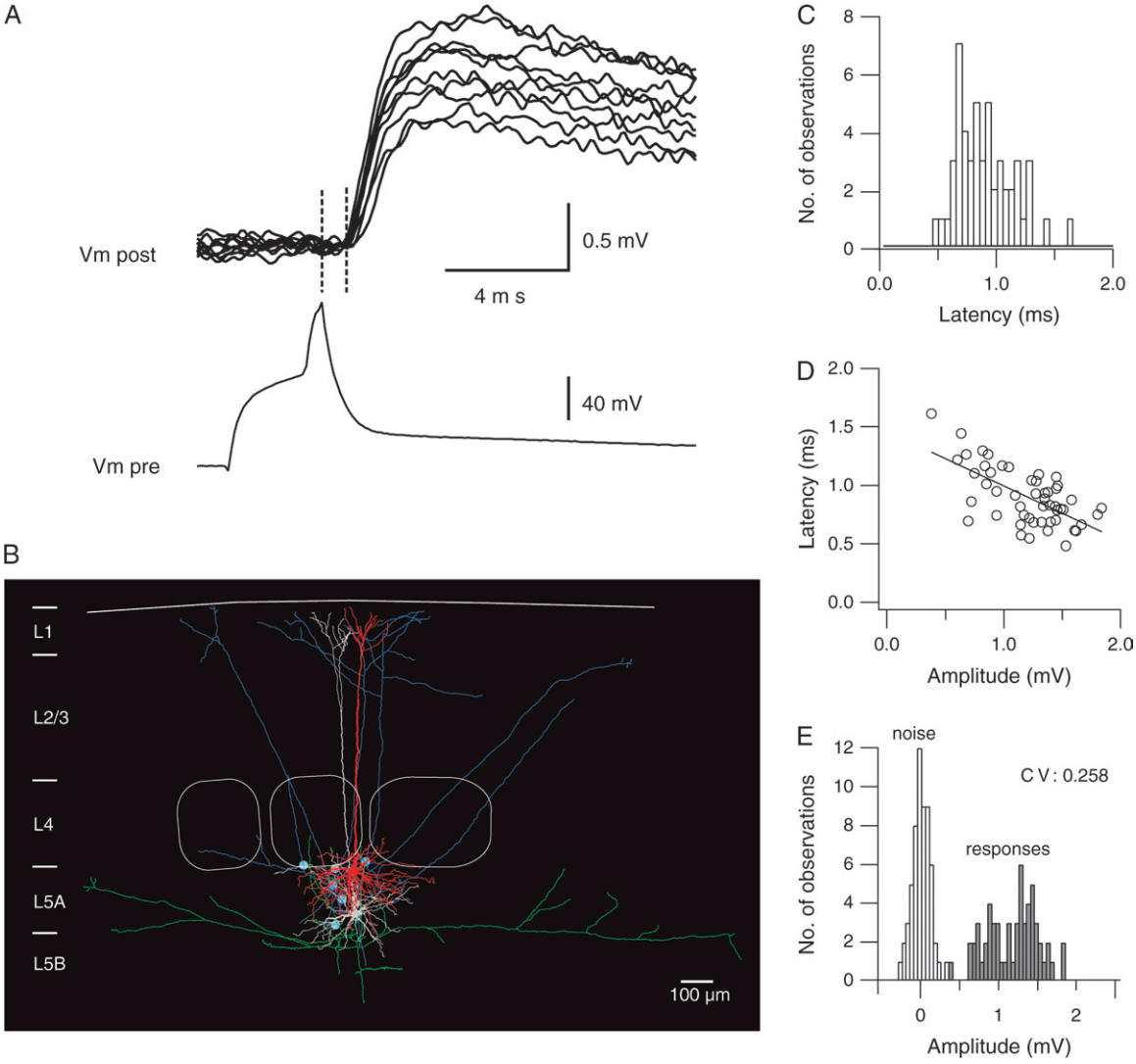

Figure 5. Latency and amplitude fluctuations of unitary EPSPs. Example of unitary EPSPs recorded from a monosynaptic L5A–L5A connection. (*A*) Ten consecutive EPSPs recorded in the postsynaptic pyramidal neuron elicited by an AP in the presynaptic neuron. The dotted lines indicate the latency of the response, measured from the peak of the presynaptic AP to the beginning of the EPSP. (*B*) The reconstruction of this pair shows the location of the putative synaptic contacts at different distances from the soma. (*C*) Histogram of the latencies for this connection. (*D*) Latencies were inversely correlated with the amplitude of the responses. (*E*) Histogram of the amplitudes of the responses and the background voltage noise showing a clear separation of both.

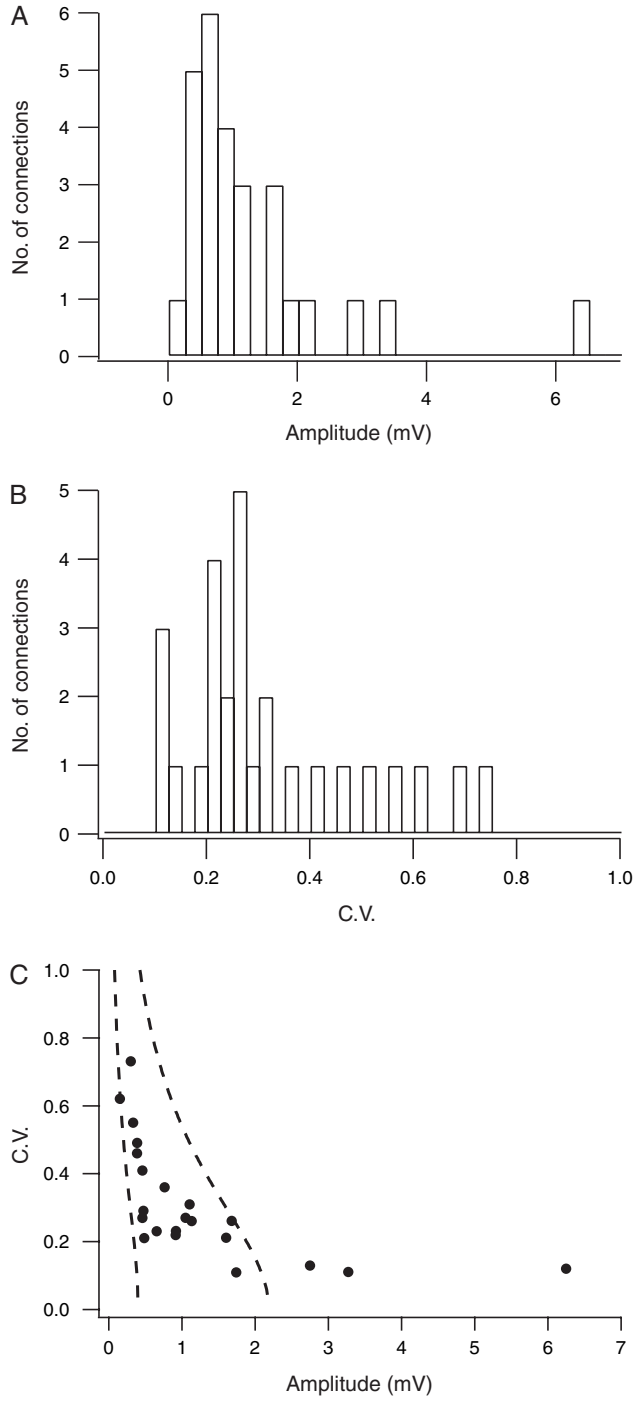

Figure 6. Average amplitude and CV of unitary EPSPs. Population data of unitary EPSPs for L5A–L5A connections. Histograms of unitary EPSP amplitude (*A*) and CV (*B*). (*C*) CV is plotted as a function of mean EPSP amplitude. The 2 dashed lines represent the predictions of single binomial release statistics for the CV as a function of EPSP amplitude assuming 4 synaptic contacts (close to average number of contacts, see Table 2) and q_s = 0.10 mV (right curve) and q_s = 0.55 mV (left curve); p_r increases from 0.08 to 0.6 (right curve) and from 0.05 to 1.0 (left curve). The p_r values refer to the 2 end points of each curve. Connections with large mean EPSP amplitudes are not well described by binomial release statistics.

pathway from VPM and the paralemniscal pathway from POm. L5A pyramidal neurons are able to integrate both streams of information at an early stage of cortical processing. Whereas POm neurons contact L5A pyramidal neurons directly (Koralek et al. 1988; Chmielowska et al. 1989; Lu and Lin 1993; Kim and Ebner 1999; Ahissar and Kleinfeld 2003; Bureau et al. 2006), VPM projects to layers 4, 5B, and upper layer 6 (Chmielowska et al. 1989; Lu and Lin 1993; Bureau et al. 2006) and indirectly reaches L5A via monosynaptic connections from L4 (Fig. 8*A*; Feldmeyer et al. 2005). Further evidence for the L4–L5A projection comes from anatomical studies showing an extensive overlap of L4 axons and L5A dendrites (Lübke et al. 2000, 2003; Brecht and Sakmann 2002) as well as physiological data (Wirth and Lüscher 2004; Schubert et al. 2006) placing L5A pyramidal cells at an early convergence point for the lemniscal and paralemniscal pathways. This is in contrast to suggestions that these pathways are largely segregated in the barrel cortex (Bureau et al. 2006). The narrow RFs of L5A pyramidal neurons (Manns et al. 2004) could be the result of L4 spiny stellate cell input (which have also a narrow RF, Brecht and Sakmann 2002) provided that this projection is stronger than those arriving from other cortical layers. Intracolumnar input to L5A pyramidal cells originates from layer 2/3 and L5B (Schubert et al. 2006) and—with a high local connectivity—from L5A (this study). In turn, L5A pyramidal neurons project to layer 2/3 (Feldmeyer et al. 2005; Shepherd et al. 2005), L5A (this study), and L5B (Schubert et al. 2001), thereby establishing reciprocal intracolumnar connections with these layers, as previously suggested for L2/3–L5A connections (Bernardo, McCasland, Woolsey, and Strominger, 1990; Gottlieb and Keller 1997; Kim and Ebner 1999). Besides these intracolumnar projections, L5A is a major output layer to other cortical (motor and secondary somatosensory) as well as subcortical (basal ganglia) areas (Donoghue and Parham 1983; Chmielowska et al. 1989; Koralek et al. 1990; Mercier et al. 1990; Lu and Lin 1993; Alloway et al. 1999, 2004; Hoffer et al. 2005).

Connectivity in L5A

Based on our data and other studies, we are now able to estimate connectivity within the network of slender-tufted L5A pyramidal neurons of a single barrel column (Fig. 8). Here, connectivity is defined as the number of L5A pyramidal neurons targeted by another single L5A pyramidal neuron and quantified accordingly. This anatomical connectivity value is subsequently adjusted to take into account the percentage of neurons actually discharging APs following whisker stimulations in vivo. We calculated connectivity as follows: The total axonal length of presynaptic L5A pyramidal neurons within the innervation domain (see Figs 2*B3* and 8*B*) was on average ~2600 μm; the axons had a bouton density of 0.4/μm axon length (see Methods) yielding a total of 1040 boutons in this region; from this value, we subtracted 10% because some boutons (5–25%; see e.g., DeFelipe and Farinas 1992; Beaulieu 1993; DeFelipe et al. 1999) form contacts with γ-aminobutyric acidergic interneurones; the corrected number was then divided by the number of putative synaptic contacts per L5A–L5A connection (~3.5 contacts). For this calculation, we took into account only monosynaptic connections established by L5A axons onto other L5A pyramidal neurons. For simplicity, we ignored potential connections with other target structures such as the dendrites of pyramidal neurons from deeper layers, as their density in L5A is rather low (Markram et al. 1997; Zhang and Deschênes 1997; Manns et al. 2004). Thus, a single L5A pyramidal neuron will target (maximally) in the order of 270 other L5A pyramidal neurons within the local network of a barrel column. Functionally, however, this value might be lower by nearly an order of magnitude because on average only about 10–15% of L5A

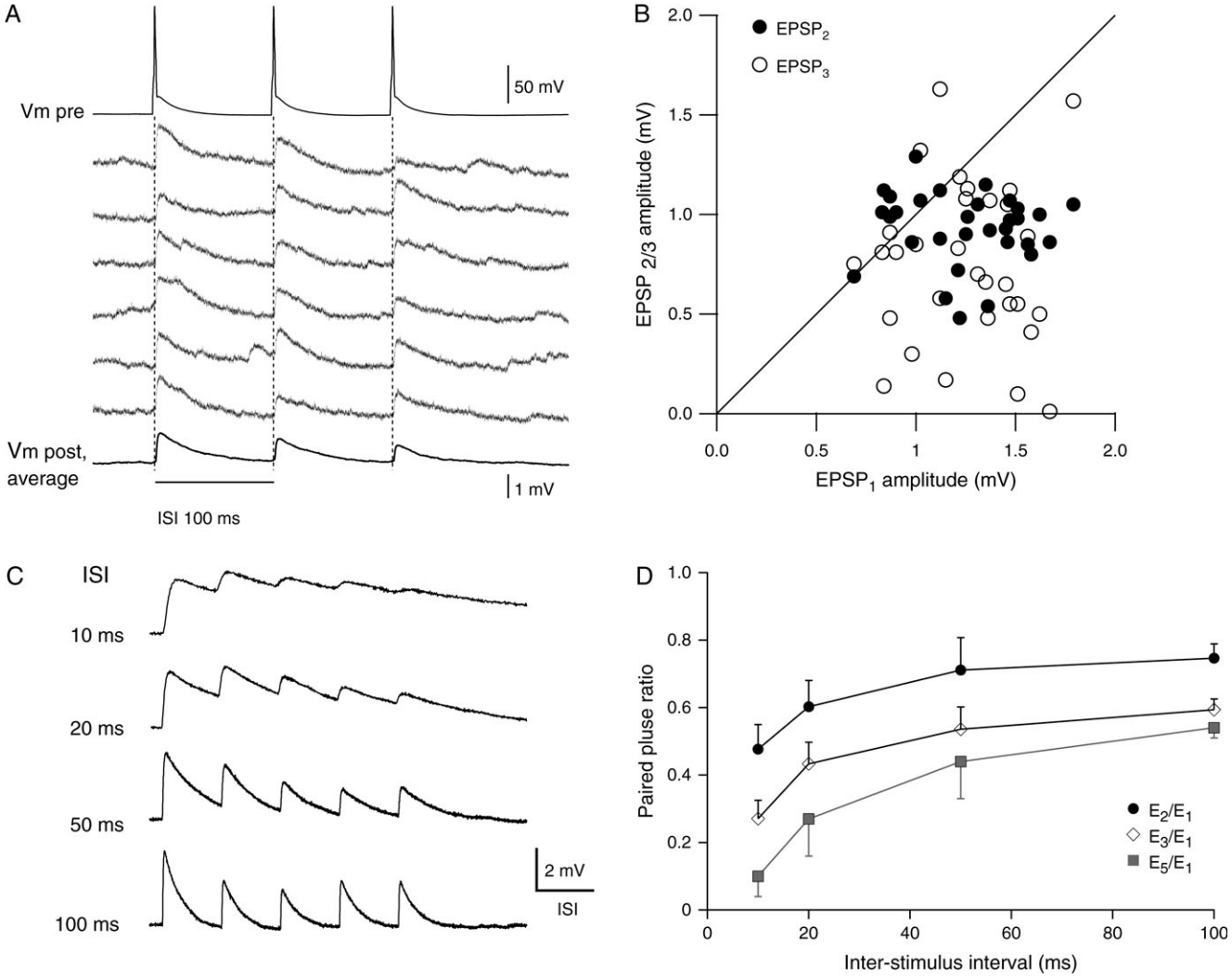

Figure 7. Short-term dynamics of unitary EPSPs. (*A*) Example of 6 successive traces recorded from the postsynaptic neuron in response to triplets of presynaptic APs with ISIs of 100 ms (top trace). The average EPSP waveform is shown at the bottom. (*B*) Same connection as in (*A*); amplitude values for $EPSP_2$ (black symbols) and $EPSP_3$ (open symbols) are plotted versus $EPSP_1$ for 30 successive sweeps. (*C*) Different L5A–L5A connection. Trains of 5 consecutive EPSPs were evoked at various interstimulus intervals as indicated on the left. EPSP amplitude depression occurred at all frequencies tested. The horizontal scale bar corresponds to the interstimulus interval of each train. (*D*) Amplitude ratios ($EPSP_2$/$EPSP_1$, filled circles; $EPSP_3$/$EPSP_1$, open squares; $EPSP_5$/$EPSP_1$, filled squares) plotted as a function of the interstimulus intervals. For short interstimulus intervals (10–50 ms), the baseline to measure EPSP amplitudes was averaged over 1–5 ms just before the stimuli for longer intervals over 10 ms.

neurons are activated by passive deflections of the principal whisker in anesthetized animals (Manns et al. 2004; de Kock et al. 2007). Nevertheless, it is conceivable that the overall activity of L5A pyramidal neurons—and therefore their impact on feed-forward excitation—is increased if the animal is awake and actively processing behaviorally relevant sensory information (Castro-Alamancos 2004).

Comparison with L4–L5A Connections

Spiny stellate cells in L4 also form monosynaptic connection with L5A pyramidal neurons (Feldmeyer et al. 2005), allowing comparison of connection properties that depend on the identity of the projecting neuron (L4 spiny stellate cell vs. L5A pyramidal neuron). At postnatal week 3, reliability (CV ~0.35) and PPR at 10 Hz (~0.8 for $EPSP_2$) are comparable for both connections, but the synaptic efficacy for the L4–L5A projection (~0.6 mV) is only ~50% that of the L5A–L5A one (~1.2 mV) measured at the same age. The weaker efficacy of the L4–L5A connection could be explained by a lower number of (putative) synaptic contacts (2.4 ± 0.9 vs. 3.5 ± 1.8 for L5A–L5A), which are also further away from the soma (~2/3 on apical dendrites vs. 2/3 on basal dendrites for L5A–L5A). This spatial segregation of inputs is reflected in the contours of their 2D innervation domains (Fig. 8*B*). However, both connections show a tendency toward a vertical clustering predominantly arranged along the lateral walls of the barrel column.

Short-Term Changes in Synaptic Efficacy

Most neocortical synapses studied so far change their efficacy in response to repetitive presynaptic APs (e.g., Thomson et al. 1993; Markram and Tsodyks 1996; Reyes and Sakmann 1999; Feldmeyer et al. 2002, 2006). These short-term changes of synaptic efficacy depend on cell identities and age (Markram et al. 1998; Reyes et al. 1998; Reyes and Sakmann 1999; Koester and Johnston 2005) and are caused by mechanisms that regulate Ca^{2+}-dependent transmitter release or synaptic response (Zucker

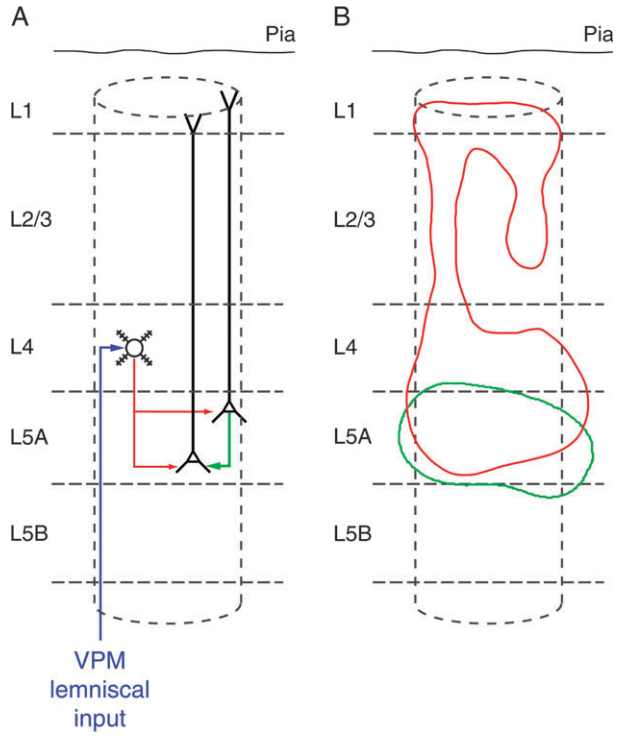

Figure 8. Connection scheme in a barrel column. (*A*) Schematic depicting a barrel column and intracortical L4–L5A and L5A–L5A connections as well as thalamocortical input from the lemniscal nucleus VPM. (*B*) Respective innervation domains (80% contour lines) for the 2 intracortical connections within the barrel column (L4–L5A connection, red; L5A–L5A connection, green). (Data for the L4–L5A connection were taken from Feldmeyer et al. 2005).

and Regehr 2002). Simplistically, synapses with a low release probability (p_r) display facilitation, whereas synapses with a high p_r exhibit depression (Thomson 2003). We found that unitary EPSPs between L5A pyramidal neurons displayed short-term depression at all frequencies (2–100 Hz) tested (~80% for the second EPSP amplitude and 70% for the third EPSP amplitude at 10 Hz). This is in accordance with previous studies on monosynaptic connections in the neocortex of young rats (2–3 weeks postnatal), which include connections between pyramidal neurons (L5B–L5B and L2/3–L5B) (Thomson et al. 1993; Markram et al. 1997; Reyes and Sakmann 1999), as well as between L4 spiny stellate cells and L5A pyramidal neurons (~80% at 10 Hz, see above; Feldmeyer et al. 2005). At discharge rates as low as or higher than 2 Hz, such short-term depression will limit the spread of activity within the network of L5A pyramidal neurons. Single APs, on the other hand, are efficiently and reliably transmitted in this juvenile intralayer cortical network. It remains to be shown whether the spread of activity in this L5A network is altered in the mature cortex.

Notes

We would like to thank Drs Tansu Celikel and Randy Bruno for comments on an earlier version of the manuscript, Dr Achim Heinz and Marcel Oberländer for help with the imaging software, and Marlies Kaiser for excellent technical assistance. This work was supported by the Max Planck Society. *Conflict of Interest*: None declared.

Address correspondence to Andreas Frick, PhD, Max-Planck-Institut für Medizinische Forschung, Abteilung Zellphysiologie, Jahnstrasse 29, 69120 Heidelberg, Germany. Email: andreas.frick@mpimf-heidelberg.mpg.de.

References

Ahissar E, Kleinfeld D. 2003. Closed-loop neuronal computations: focus on vibrissa somatosensation in rat. Cereb Cortex. 13:52–62.

Ahissar E, Sosnik R, Bagdasarian K, Haidarliu S. 2001. Temporal frequency of whisker movement. II. Laminar organization of cortical representations. J Neurophysiol. 86:354–367.

Alloway KD, Crist J, Mutic JJ, Roy SA. 1999. Corticostriatal projections from rat barrel cortex have an anisotropic organization that correlates with vibrissal whisking behavior. J Neurosci. 19:10908–10922.

Alloway KD, Zhang M, Chakrabarti S. 2004. Septal columns in rodent barrel cortex: functional circuits for modulating whisking behavior. J Comp Neurol. 480:299–309.

Armstrong-James M, Diamond ME, Ebner FF. 1994. An innocuous bias in whisker use in adult rats modifies receptive fields of barrel cortex neurons. J Neurosci. 14:6978–6991.

Banitt Y, Martin KA, Segev I. 2005. Depressed responses of facilitatory synapses. J Neurophysiol. 94:865–870.

Beaulieu C. 1993. Numerical data on neocortical neurons in adult rat, with special reference to the GABA population. Brain Res. 609:284–292.

Bernardo KL, McCasland JS, Woolsey TA. 1990. Local axonal trajectories in mouse barrel cortex. Exp Brain Res. 82:247–253.

Bernardo KL, McCasland JS, Woolsey TA, Strominger RN. 1990. Local intra- and interlaminar connections in mouse barrel cortex. J Comp Neurol. 291:231–255.

Brecht M, Roth A, Sakmann B. 2003. Dynamic receptive fields of reconstructed pyramidal cells in layers 3 and 2 of rat somatosensory barrel cortex. J Physiol. 553:243–265.

Brecht M, Sakmann B. 2002. Dynamic representation of whisker deflection by synaptic potentials in spiny stellate and pyramidal cells in the barrels and septa of layer 4 rat somatosensory cortex. J Physiol (Lond). 543 (Pt 1):49–70.

Brecht M, Schneider M, Sakmann B, Margrie TW. 2004. Whisker movements evoked by stimulation of single pyramidal neuronal cells in rat motor cortex. Nature. 427:704–710.

Bureau I, von Saint Paul F, Svoboda K. 2006. Interdigitated paralemniscal and lemniscal pathways in the mouse barrel cortex. PloS Biol. 4(12):e382.

Castro-Alamancos MA. 2004. Dynamics of sensory thalamocortical synaptic networks during information processing states. Prog Neurobiol. 74:213–247.

Chmielowska J, Carvell GE, Simons DJ. 1989. Spatial organization of thalamocortical and corticothalamic projection systems in the rat SmI barrel cortex. J Comp Neurol. 285:325–338.

DeFelipe J, Farinas I. 1992. The pyramidal neuron of the cerebral cortex: morphological and chemical characteristics of the synaptic inputs. Prog Neurobiol. 39:563–607.

DeFelipe J, Marco P, Busturia I, Merchan-Perez A. 1999. Estimation of the number of synapses in the cerebral cortex: methodological considerations. Cereb Cortex. 9:722–732.

De Kock CPJ, Bruno RM, Spors H, Sakmann B. Forthcoming 2007. Layer and cell type specific suprathreshold stimulus representation in primary somatosensory cortex. J Physiol. doi: 10.1113/jphysiol.2006.124321.

Donoghue JP, Parham C. 1983. Afferent connections of the lateral agranular field of the rat motor cortex. J Comp Neurol. 217:390–404.

Douglas RJ, Martin KA. 2004. Neuronal circuits of the neocortex. Annu Rev Neurosci. 27:419–451.

Feldmeyer D, Egger V, Lübke J, Sakmann B. 1999. Reliable synaptic connections between pairs of excitatory layer 4 neurones within a single 'barrel' of developing rat somatosensory cortex. J Physiol (Lond). 521:169–190.

Feldmeyer D, Lübke J, Sakmann B. 2006. Efficacy and connectivity of intracolumnar pairs of layer 2/3 pyramidal cells in the barrel cortex of juvenile rats. J Physiol (Lond). 575:583–602.

Feldmeyer D, Lübke J, Silver RA, Sakmann B. 2002. Synaptic connections between layer 4 spiny neurone–layer 2/3 pyramidal cell pairs in juvenile rat barrel cortex: physiology and anatomy of interlaminar signalling within a cortical column. J Physiol (Lond). 538 (Pt 3):803–822.

Feldmeyer D, Roth A, Sakmann B. 2005. Monosynaptic connections between pairs of spiny stellate cells in layer 4 and pyramidal cells in layer 5A indicate that lemniscal and paralemniscal afferent pathways converge in the infragranular somatosensory cortex. J Neurosci. 25:3423–3431.

Gottlieb JP, Keller A. 1997. Intrinsic circuitry and physiological properties of pyramidal neurons in rat barrel cortex. Exp Brain Res. 115:47–60.

Hoeflinger BF, Bennett-Clarke CA, Chiaia NL, Killackey HP, Rhoades RW. 1995. Patterning of local intracortical projections within the vibrissae representation of rat primary somatosensory cortex. J Comp Neurol. 354:551–563.

Hoffer ZS, Arantes HB, Roth RL, Alloway KD. 2005. Functional circuits mediating sensorimotor integration: quantitative comparisons of projections from rodent barrel cortex to primary motor cortex, neostriatum, superior colliculus, and the pons. J Comp Neurol. 488:82–100.

Huang W, Armstrong-James M, Rema V, Diamond ME, Ebner FF. 1998. Contribution of supragranular layers to sensory processing and plasticity in adult rat barrel cortex. J Neurophysiol. 80:3261–3271.

Ito M. 1992. Simultaneous visualization of cortical barrels and horseradish peroxidase-injected layer 5b vibrissa neurones in the rat. J Physiol. 454:247–265.

Killackey HP, Koralek KA, Chiaia NL, Rhodes RW. 1989. Laminar and areal differences in the origin of the subcortical projection neurons of the rat somatosensory cortex. J Comp Neurol. 282:428–445.

Kim U, Ebner FF. 1999. Barrels and septa: separate circuits in rat barrels field cortex. J Comp Neurol. 408:489–505.

Koester HJ, Johnston D. 2005. Target cell-dependent normalization of transmitter release at neocortical synapses. Science. 308:863–866.

Koralek KA, Jensen KF, Killackey HP. 1988. Evidence for two complementary patterns of thalamic input to the rat somatosensory cortex. Brain Res. 463:346–351.

Koralek KA, Olavarria J, Killackey HP. 1990. Areal and laminar organization of corticocortical projections in the rat somatosensory cortex. J Comp Neurol. 299:133–150.

Larsen DD, Callaway EM. 2006. Development of layer-specific axonal arborizations in mouse primary somatosensory cortex. J Comp Neurol. 494:398–414.

Lu SM, Lin RC. 1993. Thalamic afferents of the rat barrel cortex: a light- and electron-microscopic study using Phaseolus vulgaris leucoagglutinin as an anterograde tracer. Somatosens Mot Res. 10:1–16.

Lübke J, Egger V, Sakmann B, Feldmeyer D. 2000. Columnar organization of dendrites and axons of single and synaptically coupled excitatory spiny neurons in layer 4 of the rat barrel cortex. J Neurosci. 20:5300–5311.

Lübke J, Roth A, Feldmeyer D, Sakmann B. 2003. Morphometric analysis of the columnar innervation domain of neurons connecting layer 4 and layer 2/3 of juvenile rat barrel cortex. Cereb Cortex. 13:1051–1063.

Manns ID, Sakmann B, Brecht M. 2004. Sub- and suprathreshold receptive field properties of pyramidal neurones in layers 5A and 5B of rat somatosensory barrel cortex. J Physiol (Lond). 556:601–622.

Markram H, Lübke J, Frotscher M, Roth A, Sakmann B. 1997. Physiology and anatomy of synaptic connections between thick tufted pyramidal neurons in the developing rat neocortex. J Physiol (Lond). 500:409–440.

Markram H, Tsodyks M. 1996. Redistribution of synaptic efficacy: a mechanism to generate infinite synaptic input diversity from a homogeneous population of neurons without changing absolute synaptic efficacies. J Physiol (Paris). 90:229–232.

Markram H, Wang Y, Tsodyks M. 1998. Differential signalling via the same axon of neocortical pyramidal neurons. Proc Natl Acad Sci USA. 95:5323–5328.

Mercier BE, Legg CR, Glickstein M. 1990. Basal ganglia and cerebellum receive different somatosensory information in rats. Proc Natl Acad Sci USA. 87:4388–4392.

Nelson S. 2002. Cortical microcircuits: diverse or canonical? Neuron. 36:19–27.

Reyes A, Lujan R, Rozov A, Burnashev N, Somogyi P, Sakmann B. 1998. Target-cell-specific facilitation and depression in neocortical circuits. Nat Neurosci. 1:279–285.

Reyes A, Sakmann B. 1999. Developmental switch in the short-term modification of unitary EPSPs evoked in layer 2/3 and layer 5 pyramidal neurons of rat neocortex. J Neurosci. 19:3827–3835.

Schubert D, Kötter R, Luhmann HJ, Staiger JF. 2006. Morphology, electrophysiology and functional input connectivity of pyramidal neurons characterizes a genuine layer Va in the primary somatosensory cortex. Cereb Cortex. 16:223–236.

Schubert D, Staiger JF, Cho N, Kötter R, Zilles K, Luhmann HJ. 2001. Layer specific intracolumnar and transcolumnar functional connectivity of layer V pyramidal cells in rat barrel cortex. J Neurosci. 21:3580–3592.

Shepherd MG, Stepanyants A, Bureau I, Chklovskii D, Svoboda K. 2005. Geometric and functional organization of cortical circuits. Nat Neurosci. 8:782–790.

Thomson AM. 2003. Presynaptic frequency- and pattern-dependent filtering. J Comput Neurosci. 15:159–202.

Thomson AM, Deuchars J, West DC. 1993. Large, deep layer pyramid-pyramid single axon EPSPs in slices of rat motor cortex display paired pulse and frequency-dependent depression, mediated presynaptically and self-facilitation, mediated postsynaptically. J Neurophysiol. 70:2354–2369.

Wilent WB, Contreras D. 2004. Synaptic responses to whisker deflections in rat barrel cortex as a function of cortical layer and stimulus intensity. J Neurosci. 24:3985–3998.

Wirth C, Lüscher HR. 2004. Spatiotemporal evolution of excitation and inhibition in the rat barrel cortex investigated with multielectrode arrays. J Neurophysiol. 91:1635–1647.

Wise SP, Jones EG. 1977. Cells of origin and terminal distribution of descending projections of the rat somatic sensory cortex. J Comp Neurol. 175:129–157.

Woolsey TA, van der Loos H. 1970. The structural organization of layer IV in the somatosensory region (SI) of mouse cerebral cortex. The description of a cortical field composed of discrete cytoarchitectonic units. Brain Res. 17:205–242.

Zhang Z-W, Deschênes M. 1997. Intracortical axonal projections of lamina VI cells of the primary somatosensory cortex in the rat: a single-cell labeling study. J Neurosci. 17:6365–6379.

Zilles K, Wree A. 1995. Cortex: areal and laminar structure. In: Paxinos G, editor. The rat nervous system. New York: Academic Press. p. 649–685.

Zucker RS, Regehr WG. 2002. Short-term synaptic plasticity. Annu Rev Physiol. 64:355–405.